

Coupling effect on the occurrence of partial synchronization in four coupled chaotic systems

Woochang Lim, Sang-Yoon Kim *

Department of Physics, Kangwon National University, Chunchon, Kangwon-Do 200-701, Republic of Korea

Received 16 September 2005; received in revised form 13 December 2005; accepted 14 December 2005

Available online 11 January 2006

Communicated by C.R. Doering

Abstract

We study the coupling effect on the occurrence of partial synchronization in four coupled one-dimensional maps by varying a parameter w ($0 \leq w \leq 1$) which tunes the “weight” in the next-nearest-neighbor coupling from the local nearest-neighbor coupling ($w = 0$) to the global coupling ($w = 1$). As the coupling parameter ε decreases and passes a threshold value ε^* , the fully synchronized attractor on the diagonal becomes transversely unstable via a blowout bifurcation, and then a partially synchronized or completely desynchronized attractor appears depending on the value of w . For the case of local coupling ($w = 0$), partial synchronization occurs on an invariant plane. However, as w increases and passes a threshold value w^* , a transition from partial synchronization to complete desynchronization takes place. Thus, for $w^* < w \leq 1$, a fully desynchronized attractor, occupying a finite four-dimensional volume, appears. The dynamical mechanism for the occurrence of partial synchronization is investigated through competition between the laminar and bursting components of the intermittent two-cluster state born via the blowout bifurcation. Another type of partial synchronization, which occurs through a dynamical stabilization of an unstable orbit, is also discussed for both the local and global couplings. These results for the partial synchronization are also confirmed in a system of four coupled pendula.

© 2006 Elsevier B.V. All rights reserved.

PACS: 05.45.Xt

Keywords: Coupling effect; Partial synchronization; Coupled chaotic systems

1. Introduction

Recently, synchronization in coupled chaotic systems has become a field of intensive study due to its potential applications [1]. When the coupling is sufficiently strong, complete synchronization occurs (i.e., a fully synchronized attractor exists on an invariant synchronization subspace) [2]. However, as the coupling strength decreases and passes a threshold value, the fully synchronized attractor loses its stability against a perturbation transverse to the synchronization subspace, and then an asynchronous attractor may appear via a supercritical blowout bifurcation [3,4]. For this case, partial synchronization, where some of the subsystems synchronize while others do not,

or complete desynchronization may occur for three or more coupled systems [5–10]. Particularly, the partial synchronization (or clustering) has been extensively investigated in globally coupled systems where each subsystem is coupled to all the other ones with equal strength [11].

Here, we are interested in whether the asynchronous attractor born via a blowout bifurcation of the fully synchronized attractor is partially synchronized or completely desynchronized. Particularly, we are concerned about the dependence of the type of the asynchronous attractor on the coupling. An example of partial synchronization was reported in the case of local coupling [9], while another example of complete desynchronization was given for the case of global coupling [11]. These previous results show that occurrence of partial synchronization depends on the type of coupling. However, the dynamical origin for such coupling effect on the occurrence of partial synchronization remains unclear.

* Corresponding author.
E-mail addresses: wclim@kangwon.ac.kr (W. Lim),
sykim@kangwon.ac.kr (S.-Y. Kim).

This Letter is organized as follows. As a simple model to interpolate between the local and global couplings, we consider four coupled one-dimensional (1D) maps with a parameter w ($0 \leq w \leq 1$) tuning the weight of the next-nearest-neighbor coupling from the local nearest-neighbor coupling ($w = 0$) to the global coupling ($w = 1$). In Section 2, by increasing the parameter w from 0 to 1, the dynamical mechanism for the occurrence of partial synchronization is investigated through a method developed in [12] where the effect of the asymmetry in the coupling on the occurrence of partial synchronization has been studied in three coupled chaotic systems. An asynchronous two-cluster state appears on an invariant plane via a supercritical blowout bifurcation of the fully synchronized attractor. A typical trajectory in the newly-born two-cluster state exhibits on–off intermittency [13–16], where long episodes of laminar (i.e., nearly synchronous) evolution near the diagonal are occasionally interrupted by short-term bursts. When the parameter w is less than a threshold value w^* (i.e., $0 \leq w < w^*$), the two-cluster state on the invariant plane is transversely stable, and hence partial synchronization occurs. However, for $w > w^*$ a completely desynchronized attractor, occupying a four-dimensional (4D) finite volume, appears, because the two-cluster state is transversely unstable. Such transverse stability of the intermittent two-cluster state may be understood via competition between its laminar and bursting components. When the laminar (bursting) component is dominant, partial synchronization (complete desynchronization) occurs through the supercritical blowout bifurcation. With further decrease in the coupling strength, the subsequent dynamics following the above partial synchronization or complete desynchronization is also discussed. To confirm the above results, we also investigate the partial synchronization in four coupled pendula by varying the weighting factor w for the next-nearest-neighbor coupling, and find similar results. Finally, we give a summary in Section 3.

2. Coupling effect on the occurrence of partial synchronization

We investigate the coupling effect on the occurrence of partial synchronization in four coupled 1D maps T with a periodic boundary condition:

$$T : \quad x_m(t+1) = f(x_m(t)) + \frac{\varepsilon}{3+w} [f(x_{m-1}(t)) + f(x_{m+1}(t)) + wf(x_{m+2}(t)) - (2+w)f(x_m(t))],$$

$$m = 1, \dots, 4, \tag{1}$$

where $x_m(t)$ is a state variable of the m th element at a discrete time t , ε is a coupling parameter, and the uncoupled dynamics ($\varepsilon = 0$) is governed by the 1D map $f(x) = 1 - ax^2$ with a control parameter a . Here, the periodic condition imposes $x_m(t) = x_{m+4}(t)$ for all m , and the parameter w tunes the weight in the next-nearest-neighbor coupling from the local nearest-neighbor coupling ($w = 0$) to the global coupling ($w = 1$) where each 1D map is coupled to all the other ones with equal strength. Thus, the interpolation between the lo-

cal and global couplings is made through variation of w . For the case of global coupling with $w = 1$, the coupled map T has a permutation symmetry because it is invariant under exchange of any two elements ($x_k \leftrightarrow x_m$), while for the case of non-global coupling with $0 \leq w < 1$, T has a cyclic permutation symmetry because it is invariant under the cyclic permutation, $\pi(x_1, \dots, x_4) = (x_2, \dots, x_1)$. In addition to the invariant diagonal where complete synchronization occurs, the following invariant planes exist, depending on w . For $0 \leq w < 1$, there are three invariant planes, Π_1 ($\equiv \{(x_1, x_2, x_3, x_4) \mid x_1 = x_2, x_3 = x_4\}$), Π_2 ($\equiv \{(x_1, x_2, x_3, x_4) \mid x_2 = x_3, x_4 = x_1\}$), and Π_3 ($\equiv \{(x_1, x_2, x_3, x_4) \mid x_1 = x_3, x_2 = x_4\}$). Here, Π_1 and Π_2 are conjugate planes with respect to the cyclic permutation, and hence dynamical states on the Π_1 and Π_2 planes have the same stability. For the case of global coupling ($w = 1$), all of the Π_1 , Π_2 , and Π_3 planes are conjugate ones with respect to the permutation. In addition to them, there exist another conjugate invariant planes for $w = 1$, Π_4 ($\equiv \{(x_1, x_2, x_3, x_4) \mid x_1, x_2 = x_3 = x_4\}$), Π_5 ($\equiv \{(x_1, x_2, x_3, x_4) \mid x_2, x_3 = x_4 = x_1\}$), Π_6 ($\equiv \{(x_1, x_2, x_3, x_4) \mid x_3, x_4 = x_1 = x_2\}$), and Π_7 ($\equiv \{(x_1, x_2, x_3, x_4) \mid x_4, x_1 = x_2 = x_3\}$). Symmetric two-cluster states (where the numbers of elements in the first and second clusters are equal) exist on the Π_1 , Π_2 , and Π_3 planes. On the other hand, asymmetric two-cluster states exist on the Π_4 , Π_5 , Π_6 , and Π_7 planes.

When the coupling parameter ε is sufficiently large, complete synchronization in which all elements become synchronized (i.e., $x_1(t) = \dots = x_4(t)$) occurs. However, as ε decreases and passes a threshold value, the fully synchronized attractor becomes transversely unstable, and then, depending on the value of w , partial synchronization or complete desynchronization may occur via a supercritical blowout bifurcation. Here, we fix the value of a at $a = 1.83$, at which a single-band chaotic attractor exists in f , and investigate the dynamical mechanism for the occurrence of partial synchronization by varying the weighting parameter w from 0 to 1.

We first consider complete synchronization occurring in the case of strong coupling. For this case, a fully synchronized attractor exists on the invariant diagonal. The longitudinal stability of a synchronized trajectory $\{x^*(t) \mid x_1(t) = x_2(t) = x_3(t) = x_4(t)\}$ on the attractor against the perturbation along the diagonal is determined by its longitudinal Lyapunov exponent

$$\sigma_{\parallel} = \lim_{L \rightarrow \infty} \frac{1}{L} \sum_{t=0}^{L-1} \ln |f'(x^*(t))|, \tag{2}$$

where the prime represents the differentiation of f with respect to x . This longitudinal Lyapunov exponent is just the Lyapunov exponent of the 1D map f , and hence it is independent of w . For $a = 1.83$, we have $\sigma_{\parallel} = 0.4765$. On the other hand, the transverse stability of the fully synchronized attractor against perturbation across the diagonal is determined by its first and second transverse Lyapunov exponents $\sigma_{\perp,1}$ ($\geq \sigma_{\perp,2}$) and $\sigma_{\perp,2}$,

$$\sigma_{\perp,1} = \sigma_{\parallel} + \ln \left| 1 - \frac{2(1+w)\varepsilon}{3+w} \right|, \tag{3}$$

$$\sigma_{\perp,2} = \sigma_{\parallel} + \ln \left| 1 - \frac{4\varepsilon}{3+w} \right|. \quad (4)$$

These transverse Lyapunov exponents, $\sigma_{\perp,1}$ with a two-fold multiplicity and $\sigma_{\perp,2}$ with no multiplicity, vary depending on w . However, for the case of global coupling ($w = 1$), the two transverse Lyapunov exponents become the same, i.e.,

$$\sigma_{\perp,1} = \sigma_{\perp,2} \equiv \sigma_{\perp} = \sigma_{\parallel} + \ln |1 - \varepsilon|, \quad (5)$$

where σ_{\perp} has a three-fold multiplicity. Plots of the transverse Lyapunov exponents versus ε for the local and global couplings are shown in Fig. 1(a) and (b), respectively. As the coupling parameter ε decreases and passes a threshold value ε_1^* (ε_2^*), $\sigma_{\perp,1}$ ($\sigma_{\perp,2}$) becomes positive. The threshold values ε_1^* and ε_2^* are denoted by the solid and dashed curves in the ε - w plane, respectively (see Fig. 1(c)), and they coincide for $w = 1$.

If ε is sufficiently large, then the first transverse Lyapunov exponent $\sigma_{\perp,1}$ is negative, and hence the fully synchronized attractor becomes transversely stable. However, as ε decreases and passes a threshold value ε_1^* , the fully synchronized attractor becomes transversely unstable because $\sigma_{\perp,1}$ becomes posi-

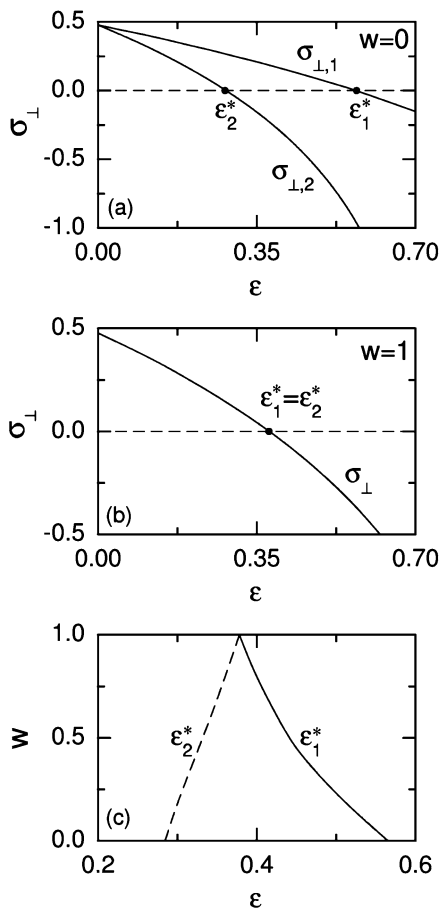


Fig. 1. Transverse stability of the fully synchronized attractor for $a = 1.83$. (a) Plots of the first and second transverse Lyapunov exponents $\sigma_{\perp,1}$ and $\sigma_{\perp,2}$ versus ε for the case of local coupling ($w = 0$). The values of $\sigma_{\perp,1}$ and $\sigma_{\perp,2}$ become positive when ε decreases and passes ε_1^* ($=0.5686$) and ε_2^* ($=0.2843$), respectively. (b) Plot of the transverse Lyapunov exponent σ_{\perp} versus ε for the case of global coupling ($w = 1$). The value of σ_{\perp} becomes positive when ε decreases and passes $\varepsilon_1^* = \varepsilon_2^*$ ($=0.3790$). (c) The threshold values of ε_1^* and ε_2^* are represented by the solid and dashed curves in the ε - w plane, respectively.

tive. Then, an asynchronous attractor, containing the diagonal, is born via a supercritical blowout bifurcation, but its type depends on the value of w . For the case of local coupling ($w = 0$), a partially synchronized attractor appears on the Π_1 plane via a supercritical blowout bifurcation, as shown in Fig. 2(a)–(f) for $\Delta\varepsilon (= \varepsilon - \varepsilon_1^*) = -0.003$. However, for the case of global coupling ($w = 1$), a completely desynchronized attractor, occupying a finite 4D volume, appears (e.g., see Fig. 2(g)–(l) for $\Delta\varepsilon = -0.003$). This complete desynchronization is in contrast to the partial synchronization for $w = 0$. Such complete desynchronization occurs because the two-cluster state on the Π_1 plane, born via the supercritical blowout bifurcation, becomes transversely unstable, as will be shown below.

When the fully synchronized attractor on the diagonal becomes transversely unstable, a (symmetric) two-cluster state appears on the invariant Π_1 plane through a supercritical blowout bifurcation. This two-cluster state satisfies $x_1(t) = x_2(t) \equiv X_t$ and $x_3(t) = x_4(t) \equiv Y_t$, and its dynamics is governed by a reduced two-dimensional (2D) map,

$$\begin{aligned} X_{t+1} &= f(X_t) + \frac{(1+w)\varepsilon}{3+w} [f(Y_t) - f(X_t)], \\ Y_{t+1} &= f(Y_t) + \frac{(1+w)\varepsilon}{3+w} [f(X_t) - f(Y_t)]. \end{aligned} \quad (6)$$

For the accuracy of numerical calculations,¹ we introduce new coordinates U and V ,

$$U_t = \frac{X_t + Y_t}{2}, \quad V_t = \frac{X_t - Y_t}{2}. \quad (7)$$

Then, the invariant diagonal is transformed into a new invariant line $V = 0$. In these new coordinates, the 2D reduced map of Eq. (6) becomes

$$\begin{aligned} U_{t+1} &= 1 - a(U_t^2 + V_t^2), \\ V_{t+1} &= 2 \left[\frac{2(1+w)\varepsilon}{3+w} - 1 \right] a U_t V_t. \end{aligned} \quad (8)$$

Fig. 3(a) and (b) shows the two-cluster states, born via supercritical blowout bifurcations, in the U - V plane for the local ($w = 0$) and global ($w = 1$) couplings, respectively. These two-cluster states are chaotic attractors in the reduced 2D map (i.e., they are chaotic attractors in the restricted Π_1 plane). Although the two-cluster states seem to be similar, their transverse stability against perturbation across the Π_1 plane depends on the value of w . Only when the two-cluster state is transversely

¹ When the magnitude of a transverse variable d of a typical trajectory in the two-cluster state, representing the deviation from the invariant synchronization line, is less than a threshold value \tilde{d} , the computed trajectory falls into an exactly synchronous state due to a finite precision. In the system of coordinates X and Y , the order of magnitude of the threshold value \tilde{d} for $d (=|X - Y|)$ is about 10^{-15} except the region near the origin, because the double-precision values of X and Y have about 15 decimal places of precision. On the other hand, in the system of U and V , the order of magnitude of the threshold value \tilde{d} for $d (=|V|)$ is about 10^{-308} , which is a threshold value for the numerical underflow in the IEEE (Institute of Electrical and Electronics Engineers) double-precision calculation. Hence, in the system of U and V , we can follow a trajectory until its length becomes sufficiently long for the calculation of Lyapunov exponents of the two-cluster state.

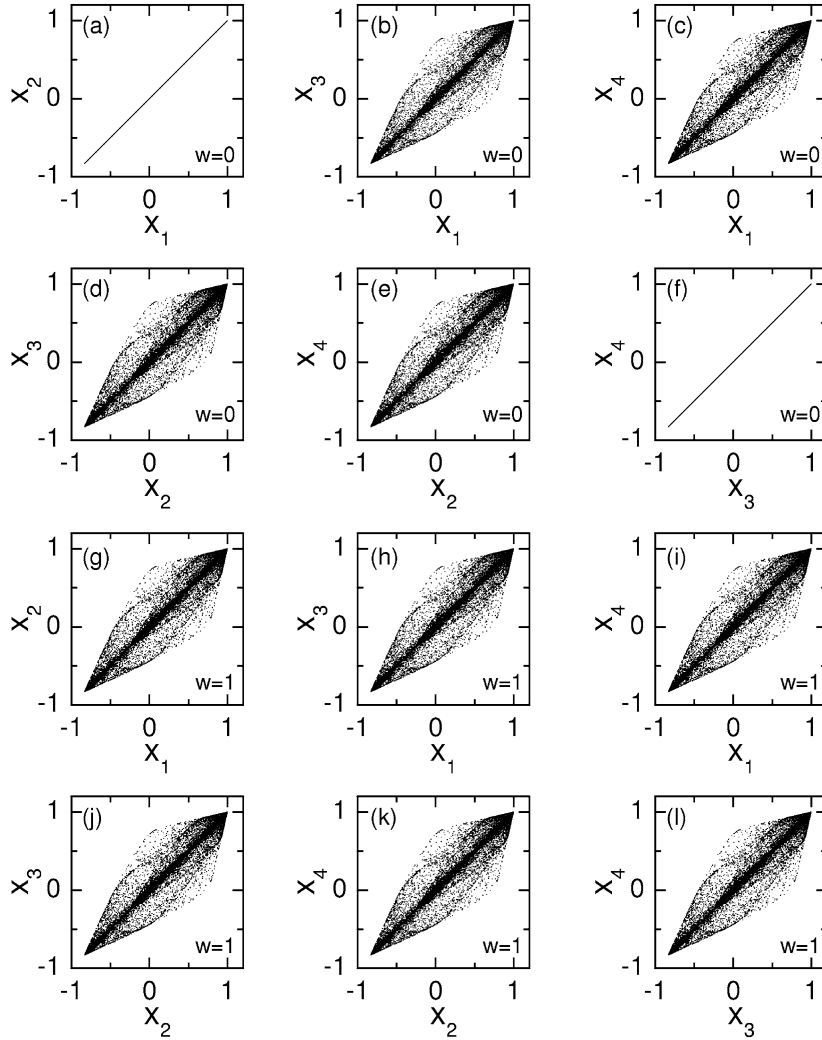


Fig. 2. (a)–(f) Projections of the partially synchronized attractor on the invariant Π_1 plane which is born via a blowout bifurcation of the fully synchronized attractor for $a = 1.83$ and $\Delta\varepsilon (= \varepsilon - \varepsilon_1^*) = -0.003$ ($\varepsilon_1^* = 0.5686$) in the case of local coupling ($w = 0$). (g)–(l) Projections of the completely desynchronized attractor born via a blowout bifurcation of the fully synchronized attractor for $a = 1.83$ and $\Delta\varepsilon = -0.003$ ($\varepsilon_1^* = 0.3790$) for the case of global coupling ($w = 1$).

stable, it becomes an attractor in the whole 4D space. To determine the transverse stability of a two-cluster state, we numerically follow a typical trajectory in the two-cluster state until its length L becomes 10^8 , and then, we obtain the Lyapunov exponents $\sigma_1, \sigma_2, \sigma_3$, and σ_4 ($\sigma_i \geq \sigma_{i+1}$ for $i = 1, 2, 3$) through the Gram–Schmidt reorthonormalization procedure [17]. In the region of ε we study, the first and second Lyapunov exponents correspond to the longitudinal Lyapunov exponents, $\sigma_{\parallel,1}$ and $\sigma_{\parallel,2}$, of the two-cluster state, respectively, which determine the longitudinal stability of the two-cluster state against the perturbation along the Π_1 plane. On the other hand, the third and fourth Lyapunov exponents correspond to the transverse Lyapunov exponents, $\sigma_{\perp,1}$ and $\sigma_{\perp,2}$, respectively, which determine the transverse stability of the two-cluster state against the perturbation across the Π_1 plane.

A plot of $\sigma_{\perp,1}$ versus $\Delta\varepsilon (= \varepsilon - \varepsilon_1^*)$ is given in Fig. 3(c) ($w = 0$ (up triangles), 0.66 (crosses), and 1 (down triangles)), where ε_1^* is the blowout bifurcation point of the fully synchronized attractor. For the case of local coupling ($w = 0$), the two-cluster state is transversely stable, because its first transverse

Lyapunov exponent $\sigma_{\perp,1}$ is negative, and hence partial synchronization occurs on the Π_1 plane via a supercritical blowout bifurcation (i.e., a partially synchronized attractor appears on the Π_1 plane.). On the other hand, as w is increased from 0, the value of $\sigma_{\perp,1}$ increases, eventually it becomes zero for a threshold value $w^* (\simeq 0.66)$, and then it becomes positive. Hence, for $w^* < w \leq 1$, complete desynchronization takes place through a supercritical blowout bifurcation (i.e., a completely desynchronized 4D attractor appears), because the two-cluster state on the Π_1 plane becomes transversely unstable. Fig. 3(a) and (b) for $\Delta\varepsilon = -0.003$ shows examples of the transversely stable ($\sigma_{\perp,1} = -0.0016$) and unstable ($\sigma_{\perp,1} = 0.0022$) two-cluster states for $w = 0$ and 1, respectively.

We now discuss the mechanism for the transition from partial synchronization to complete desynchronization by varying the weighting parameter w . A typical trajectory in the two-cluster state, exhibiting on–off intermittency, may be decomposed into the laminar (i.e., nearly synchronous) and bursting components. We use a small quantity d^* for the threshold value of the magnitude of the transverse variable $d (= |V|)$ such that

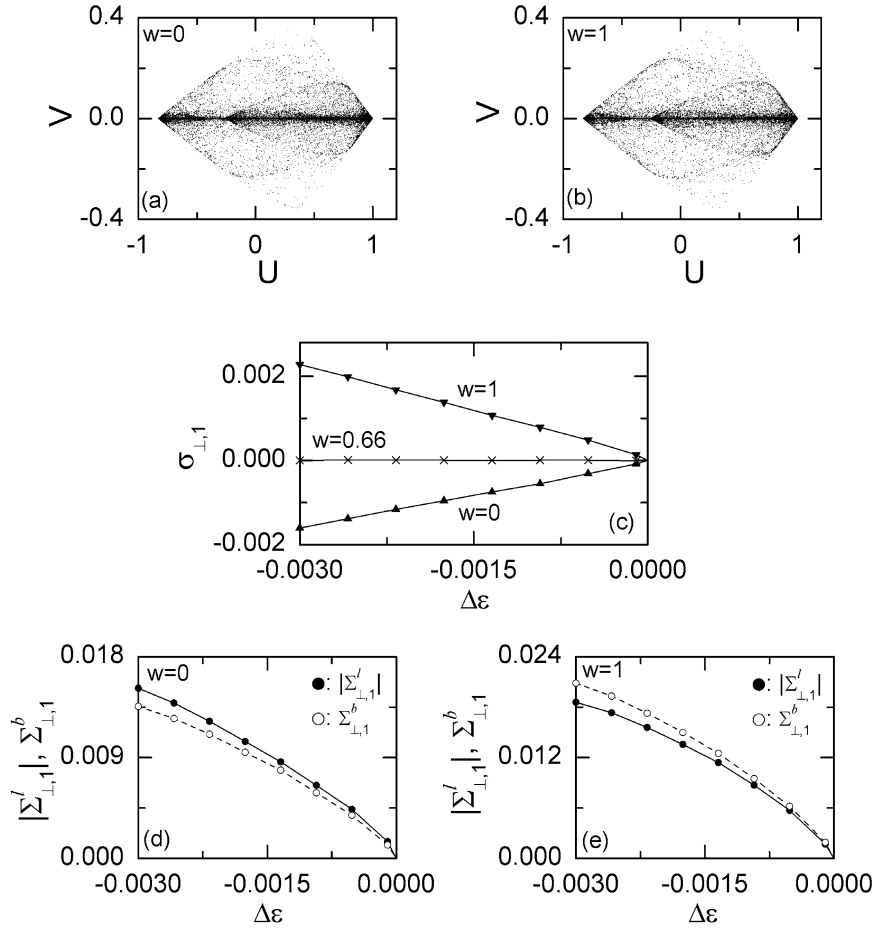


Fig. 3. (a) Transversely stable ($\sigma_{\perp,1} = -0.0016$) two-cluster state for $w = 0$ and (b) transversely unstable ($\sigma_{\perp,1} = 0.0022$) two-cluster state for $w = 1$ in the U - V plane when $a = 1.83$ and $\Delta\epsilon$ ($= \epsilon - \epsilon_1^*$) $= -0.003$. Here, the values of ϵ_1^* for $w = 0, 0.66$, and 1 are $0.5686, 0.4179$, and 0.3790 , respectively. (c) Plot of $\sigma_{\perp,1}$ (first transverse Lyapunov exponent of the two-cluster state) versus $\Delta\epsilon$ for $a = 1.83$ ($w = 0$ (up triangles), 0.66 (crosses), 1 (down triangles)). The weighted first transverse Lyapunov exponents for the laminar and bursting components, $\Sigma_{\perp,1}^l$ and $\Sigma_{\perp,1}^b$, are shown in (d) and (e) for the local ($w = 0$) and global ($w = 1$) couplings, respectively.

for $d < d^*$ the trajectory is considered to be in the laminar (off) state, while for $d > d^*$ it is considered to be in the bursting (on) state. Then, transverse stability of the intermittent two-cluster state may be determined through competition of the laminar and bursting components [12]. Its first transverse Lyapunov exponent $\sigma_{\perp,1}$ can be given by the sum of the two weighted first transverse Lyapunov exponents of the laminar and bursting components, $\Sigma_{\perp,1}^l$ and $\Sigma_{\perp,1}^b$:

$$\sigma_{\perp,1} = \Sigma_{\perp,1}^l + \Sigma_{\perp,1}^b = \Sigma_{\perp,1}^b - |\Sigma_{\perp,1}^l|, \quad (9)$$

where the laminar component always has a negative weighted first transverse Lyapunov exponent ($\Sigma_{\perp,1}^l < 0$). For each component ($i = l, b$), the weighted first transverse Lyapunov exponent $\Sigma_{\perp,1}^i$ is given by the product of the fraction, μ_i , of time spent in the i state and the first transverse Lyapunov exponent of the i th component $\sigma_{\perp,1}^i$, i.e.,

$$\Sigma_{\perp,1}^i = \mu_i \sigma_{\perp,1}^i, \quad \mu_i = \frac{L_i}{L}, \quad (10)$$

where L_i is the time spent in the i state for a trajectory segment of length L ($=10^8$). Then, the sign of $\sigma_{\perp,1}$ may be determined through competition between the laminar and bursting components

(see Eq. (9)). When the “transverse strength” of the laminar component (i.e., the magnitude of the weighted first transverse Lyapunov exponent $|\Sigma_{\perp,1}^l|$) is larger (smaller) than that of the bursting component (i.e., $\Sigma_{\perp,1}^b$), partial synchronization (complete desynchronization) occurs because the two-cluster state becomes transversely stable (unstable). Fig. 3(d) and (e) shows the weighted first transverse Lyapunov exponents of the laminar and bursting components for $w = 0$ and 1 , respectively, when the threshold value for the laminar state is $d^* = 10^{-4}$.² For the case of local coupling ($w = 0$), partial synchronization occurs on the conjugate Π_1 and Π_2 planes because the lami-

² The weighted first transverse Lyapunov exponents $\Sigma_{\perp,1}^l$ and $\Sigma_{\perp,1}^b$ of the laminar and bursting components depend on the threshold value d^* for the laminar state, while the first transverse Lyapunov exponent $\sigma_{\perp,1}$ of the two-cluster state is independent of d^* . As d^* is decreased, $\Sigma_{\perp,1}^l$ decreases to zero because the fraction μ_l of the time spent in the laminar state goes to zero; thus $\Sigma_{\perp,1}^b$ ($= \sigma_{\perp,1} + |\Sigma_{\perp,1}^l|$) converges to $\sigma_{\perp,1}$. However, we note that $\sigma_{\perp,1}$ depends only on the difference between $\Sigma_{\perp,1}^b$ and $|\Sigma_{\perp,1}^l|$, which is independent of d^* (see Eq. (9)). Hence, although $\Sigma_{\perp,1}^{l(b)}$ depends on d^* , the conclusion as to the transverse stability of the two-cluster state is independent of d^* .

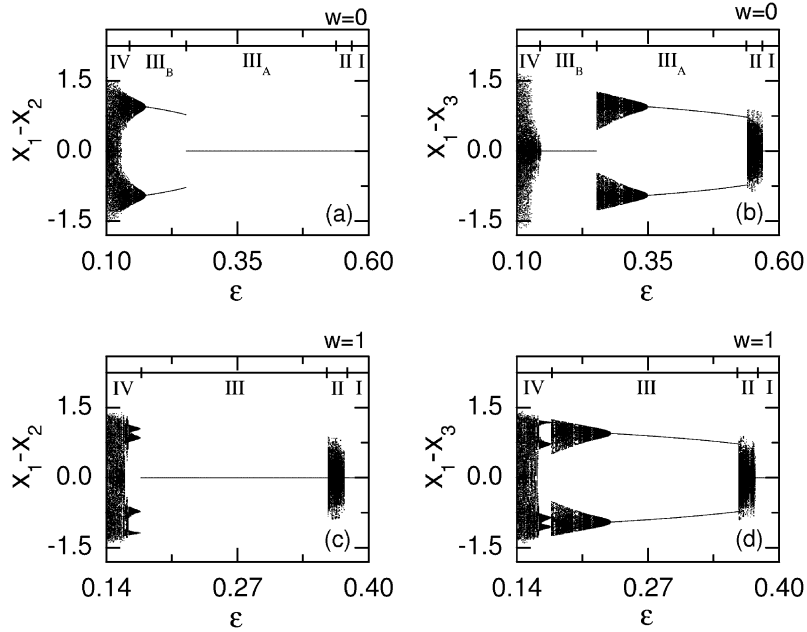


Fig. 4. Bifurcation diagrams (plots of x_1-x_2 (x_1-x_3) versus ε) when $a = 1.83$ for the cases of local coupling ((a) and (b)) and global coupling ((c) and (d)). We note that a periodic partial synchronization occurs on the Π_1 plane through a dynamic stabilization of an unstable periodic orbit in the regions III_A and III for both the local and global couplings. This partial synchronization is in contrast to the partial synchronization which occurs via a blowout bifurcation of the fully synchronized attractor. For more details on dynamical evolutions, refer to the text.

nar component is dominant (i.e., $|\Sigma_{\perp,1}^l| > \Sigma_{\perp,1}^b$ as shown in Fig. 3(d)). On the other hand, complete desynchronization takes place for the case of global coupling ($w = 1$) because the bursting component is dominant (i.e., $\Sigma_{\perp,1}^b > |\Sigma_{\perp,1}^l|$ as shown in Fig. 3(e)).

So far, we consider the blowout bifurcation of the fully synchronized attractor which occurs when passing a first threshold value ε_1^* . For this case, symmetric two-cluster states appear on the conjugate Π_1 and Π_2 planes, and their transverse stability is discussed above. As ε is further decreased and passes a second threshold value ε_2^* (see Fig. 1(c)), the second transverse Lyapunov exponent of the fully synchronized attractor becomes positive, and then another symmetric two-cluster state appears on the Π_3 plane. However, this two-cluster state on the Π_3 plane is transversely unstable for all w , and hence no partial synchronization occurs on the Π_3 plane. Furthermore, in the case of global coupling ($w = 1$), asymmetric two-cluster states appear on the conjugate Π_4, Π_5, Π_6 , and Π_7 planes when passing ε_1^* (i.e., through the blowout bifurcation of the fully synchronized attractor). However, they are also transversely unstable, and hence no partial synchronization takes place on the Π_4, Π_5, Π_6 , and Π_7 planes. Consequently, partial synchronization may occur only on the conjugate Π_1 and Π_2 planes via the blowout bifurcation, depending on w .

By decreasing ε furthermore, we briefly discuss the dynamics following the above partial synchronization or complete desynchronization. Fig. 4(a)–(d) shows the bifurcation diagrams for both cases of $w = 0$ and 1. In the region I of ε , complete synchronization occurs on the diagonal. In the region II, through the blowout bifurcation of the fully synchronized attractor, a partially synchronized attractor appears on the Π_1 plane for the case of $w = 0$, while complete desynchronization

occurs for the case of $w = 1$. However, an unstable period-2 orbit embedded in the two-cluster state on the Π_1 plane becomes stabilized through a subcritical pitchfork bifurcation for both cases of $w = 0$ and 1 (i.e., dynamic stabilization of an unstable orbit occurs). Thus, periodic partial synchronization begins on the Π_1 plane. We note that the dynamical origin of this partial synchronization is in contrast with that of the partial synchronization via the blowout bifurcation of the fully synchronized attractor. For the case of $w = 0$, such a partially synchronized periodic attractor is evolved into the quasiperiodic and chaotic attractors in the region III_A . Eventually, this partially synchronized attractor on the Π_1 plane becomes transversely unstable, and then a jump to another partially synchronized periodic attractor on the Π_3 plane occurs in the region III_B . Similar dynamical evolutions are made on the Π_1 plane in the region III for $w = 1$. Such partially synchronized attractors in the regions III_B and III also lose their transverse stability, and then complete desynchronization occurs in the region IV for both cases of $w = 0$ and 1.

To confirm the above results, we also study a system of four coupled pendula:

$$\begin{aligned} \dot{x}_m &= y_m, \\ \dot{y}_m &= f(x_m, y_m, t) \\ &\quad + \frac{\varepsilon}{3+w} [y_{m-1} + y_{m+1} + w y_{m+2} - (2+w)y_m], \end{aligned} \quad (11)$$

where $z_m = (x_m, y_m)$ ($m = 1, 2, 3, 4$) is a state vector of the m th subsystem ($z_m = z_{m+4}$ due to the periodic boundary condition),

$$f(x, y, t) = -2\pi\beta\Omega y - 2\pi(\Omega^2 - A \cos 2\pi t) \sin 2\pi x,$$

x is a normalized angle with range $x \in [0, 1)$, y is a normalized angular velocity, the overdot denotes a derivative with respect to

time t , β is a normalized damping parameter, Ω is a normalized natural frequency of the unforced pendulum, A is a normalized driving amplitude of the vertical oscillation of the suspension point, and ε is a coupling parameter. As in the coupled 1D maps of Eq. (1), w represents a weighting factor for the next-nearest-neighbor coupling (the case of $w = 0$ (1) corresponds to the local nearest-neighbor (global) coupling).

By stroboscopically sampling the orbit points at the discrete time n (i.e., $t = n$, n : integers), we obtain the eight-dimensional (8D) Poincaré map P . As an example, we consider the 8D Poincaré map for the case of $\beta = 0.5$, $\Omega = 0.5$, and $A = 0.5$. For a sufficiently large ε , a complete synchroniza-

tion (i.e., $z_1 = z_2 = z_3 = z_4$) occurs on the invariant diagonal. However, as ε decreases and passes a threshold value, the fully synchronized attractor loses its transverse stability, and then, through a supercritical blowout bifurcation, a two-cluster state appears on the Π_1 plane where $z_1 = z_2 \equiv Z_1 (= (X_1, Y_1))$ and $z_3 = z_4 \equiv Z_2 (= (X_2, Y_2))$. The dynamics of this two-cluster state is governed by a system of equations

$$\begin{aligned} \dot{X}_1 &= Y_1, & \dot{Y}_1 &= f(X_1, Y_1, t) + \frac{(1+w)\varepsilon}{3+w}(Y_2 - Y_1), \\ \dot{X}_2 &= Y_2, & \dot{Y}_2 &= f(X_2, Y_2, t) + \frac{(1+w)\varepsilon}{3+w}(Y_1 - Y_2). \end{aligned} \quad (12)$$

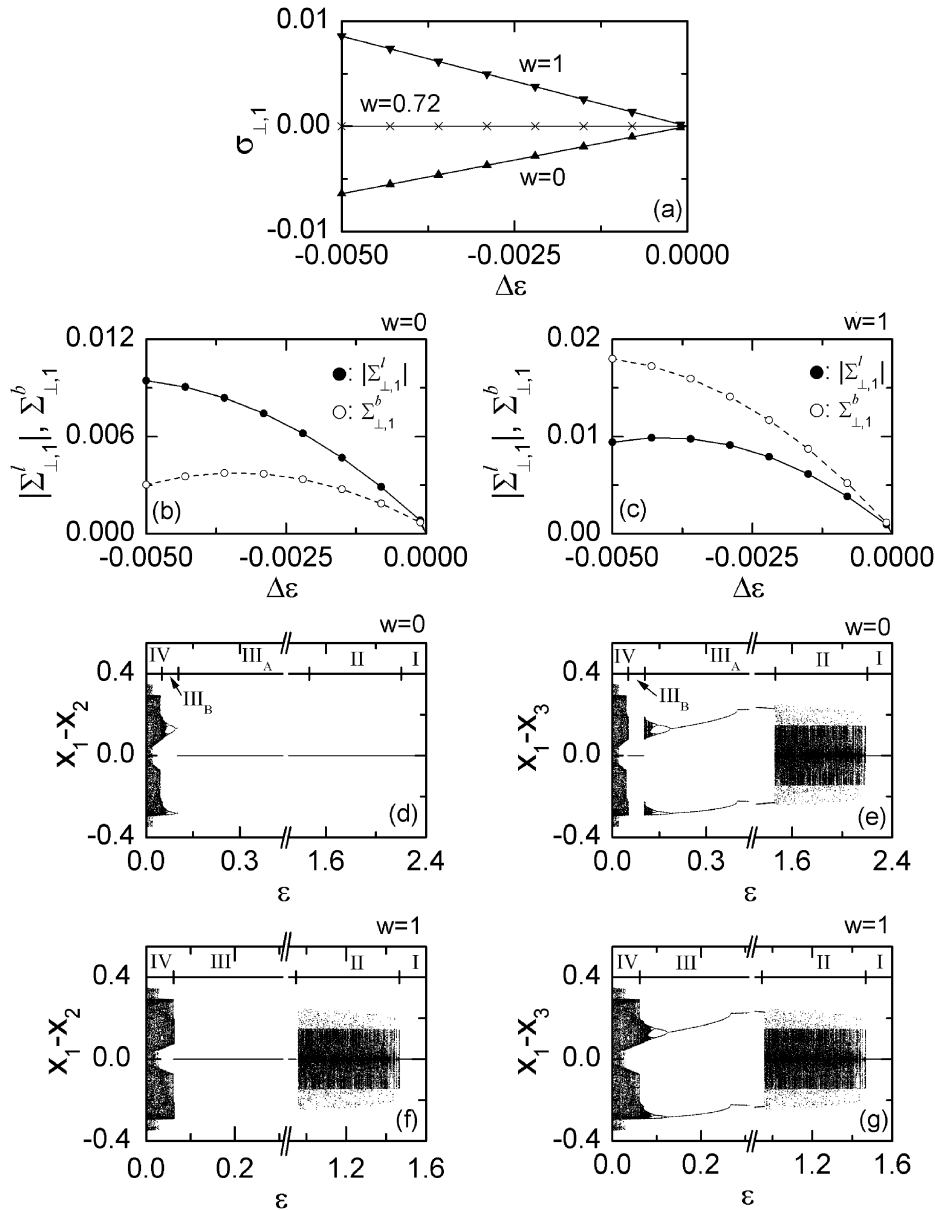


Fig. 5. Consequence of blowout bifurcations in four coupled pendula for $\beta = 0.5$, $\Omega = 0.5$, and $A = 0.5$. (a) Plot of $\sigma_{\perp,1}$ (first transverse Lyapunov exponent of the two-cluster state) versus $\Delta\varepsilon$ ($\varepsilon - \varepsilon_1^*$) ($w = 0$ (up triangles), 0.72 (crosses), 1 (down triangles)). Here, the values of ε_1^* for $w = 0, 0.72$, and 1 are 2.202, 1.617, and 1.467, respectively. The weighted first transverse Lyapunov exponents for the laminar and bursting components, $|\Sigma_{\perp,1}^l|$ and $\Sigma_{\perp,1}^b$, are shown in (b) and (c) for the local ($w = 0$) and global ($w = 1$) cases, respectively. Bifurcation diagrams (plots of $x_1 - x_2$ ($x_1 - x_3$) versus ε) for the cases of local coupling ((d) and (e)) and global coupling ((f) and (g)). A periodic partial synchronization occurs on the Π_1 plane through dynamic stabilization of an unstable periodic orbit in the regions III_A and III for both the local and global couplings. This partial synchronization is in contrast with the partial synchronization which occurs via a blowout bifurcation of the fully synchronized attractor. For more details on dynamical evolutions, refer to the text.

As in the case of coupled 1D maps, for the numerical accuracy we follow a typical trajectory in the two-cluster state until its length L becomes 10^7 , using the new coordinates,

$$\begin{aligned} U_1 &= \frac{X_1 + X_2}{2}, & U_2 &= \frac{Y_1 + Y_2}{2}, \\ V_1 &= \frac{X_1 - X_2}{2}, & V_2 &= \frac{Y_1 - Y_2}{2}. \end{aligned} \quad (13)$$

Thus, we get the eight Lyapunov exponents ($\sigma_1 \geq \dots \geq \sigma_8$) of the two-cluster state to determine its transverse stability in the whole 8D space through the Gram–Schmidt reorthonormalization procedure. For the values of ε we study, $\sigma_1, \sigma_2, \sigma_7$, and σ_8 correspond to the longitudinal Lyapunov exponents, $\sigma_{\parallel,1}, \sigma_{\parallel,2}, \sigma_{\parallel,3}$, and $\sigma_{\parallel,4}$, of the two-cluster state, while $\sigma_3, \sigma_4, \sigma_5$, and σ_6 correspond to the transverse Lyapunov exponents, $\sigma_{\perp,1}, \sigma_{\perp,2}, \sigma_{\perp,3}$, and $\sigma_{\perp,4}$, respectively.

Fig. 5(a) shows a plot of $\sigma_{\perp,1}$ versus $\Delta\varepsilon (= \varepsilon - \varepsilon_1^*)$ ($w = 0$ (up triangles), 0.72 (crosses), and 1 (down triangles)), where ε_1^* is the blowout bifurcation point of the fully synchronized attractor which exists in the region I of Fig. 5(d)–(g). For the case of local coupling ($w = 0$), partial synchronization occurs on the Π_1 plane in the region II of Fig. 5(d)–(e) because the two-cluster state is transversely stable (i.e., $\sigma_{\perp,1} < 0$). On the other hand, as w is increased from 0 and passes a threshold value w^* ($\simeq 0.72$), $\sigma_{\perp,1}$ becomes positive. Consequently, for $w^* < w \leq 1$, complete desynchronization occurs through the blowout bifurcation (e.g., see the region II of Fig. 5(f)–(g) for $w = 1$) because the two-cluster state on the Π_1 plane is transversely unstable (i.e., $\sigma_{\perp,1} > 0$). As in the case of coupled 1D maps, the transverse stability of a two-cluster state may be determined through the competition between its laminar and bursting components (see Eq. (9)). Fig. 5(b) and (c) shows the strength of the laminar and bursting components, $|\Sigma_{\perp,1}^l|$ and $\Sigma_{\perp,1}^b$ for $w = 0$ and 1, respectively, when the threshold value for the laminar state is $d^* = 10^{-4}$. For the locally coupled case ($w = 0$), the laminar component is dominant (i.e., $|\Sigma_{\perp,1}^l| > \Sigma_{\perp,1}^b$), and hence a partially synchronized attractor appears on the Π_1 plane. On the other hand, for the globally coupled case, a completely desynchronized attractor, occupying a finite 8D volume, appears because the bursting component is dominant (i.e., $\Sigma_{\perp,1}^b > \Sigma_{\perp,1}^l$). Like the case of coupled 1D maps, with further decrease in ε , another type of partial synchronization occurs through dynamic stabilization of an unstable periodic orbit (embedded in the chaotic two-cluster states). For the case of $w = 0$, this kind of partial synchronization occurs on the Π_1 plane in the region III_A of Fig. 5(d) and (e). After this partially synchronized attractor becomes transversely unstable, a jump to another partially synchronized periodic attractor on the Π_3 plane, where $z_1 = z_3$ and $z_2 = z_4$, occurs in the region III_B. For the case of $w = 1$, similar partial synchronization also occurs on the Π_1 plane in the region III of Fig. 5(f)–(g). After these partially synchronized attractors in the regions III_B and III lose their transverse stability, complete desynchronization occurs in the region IV for both cases of $w = 0$ and 1.

3. Summary

We have investigated the coupling effect on the occurrence of partial synchronization via a blowout bifurcation of the fully synchronized attractor in the four coupled 1D maps with a parameter w tuning the weight of the next-nearest-neighbor coupling. The variation of w ($0 \leq w \leq 1$) interpolates between the local ($w = 0$) and global ($w = 1$) couplings. For the case of local coupling ($w = 0$), a partially synchronized attractor appears on an invariant plane. However, as w is increased and passes a threshold value w^* ($\simeq 0.66$), a transition from partial synchronization to complete desynchronization occurs. Thus, for $w^* < w \leq 1$ a completely desynchronized attractor appears. Such a transition can be understood via competition between the laminar and bursting components of the intermittent two-cluster state born via a blowout bifurcation. If the laminar (bursting) component is dominant, then partial synchronization (complete desynchronization) occurs through the blowout bifurcation. With further decrease in the coupling strength, another type of partial synchronization, which occurs via dynamical stabilization of an unstable periodic orbit, has been found to occur for both the local and global couplings. To confirm the results for the partial synchronization, we have also studied a system of four coupled pendula, and found similar results.

Acknowledgements

This work was supported by the Korea Research Foundation (Grant No. R05-2004-000-10717-0).

References

- [1] K.M. Cuomo, A.V. Oppenheim, Phys. Rev. Lett. 71 (1993) 65; L. Kocarev, K.S. Halle, K. Eckert, L.O. Chua, U. Parlitz, Int. J. Bifur. Chaos Appl. Sci. Eng. 2 (1992) 973; L. Kocarev, U. Parlitz, Phys. Rev. Lett. 74 (1995) 5028; N.F. Rulkov, Chaos 6 (1996) 262.
- [2] H. Fujisaka, T. Yamada, Prog. Theor. Phys. 69 (1983) 32; A.S. Pikovsky, Z. Phys. B: Condens. Matter 50 (1984) 149; V.S. Afraimovich, N.N. Verichev, M.I. Rabinovich, Radiophys. Quantum Electron. 29 (1986) 795; L.M. Pecora, T.L. Carroll, Phys. Rev. Lett. 64 (1990) 821.
- [3] E. Ott, J.C. Sommerer, Phys. Lett. A 188 (1994) 39.
- [4] S.-Y. Kim, W. Lim, E. Ott, B. Hunt, Phys. Rev. E 68 (2003) 066203.
- [5] K. Pyragas, Phys. Rev. E 54 (1996) R4508.
- [6] M.S. Vieira, A.J. Lichtenberg, Phys. Rev. E 56 (1997) R3741.
- [7] M. Hasler, Yu. Maistrenko, O. Popovych, Phys. Rev. E 58 (1998) 6843; Yu. Maistrenko, O. Popovych, M. Hasler, Int. J. Bifur. Chaos Appl. Sci. Eng. 10 (2000) 179; A.V. Taborov, Yu. Maistrenko, E. Mosekilde, Int. J. Bifur. Chaos Appl. Sci. Eng. 10 (2000) 1051; S. Yanchuk, Yu. Maistrenko, E. Mosekilde, Chaos 13 (2003) 388.
- [8] M. Inoue, T. Kawazoe, Y. Nishi, M. Nagadome, Phys. Lett. A 249 (1998) 69.
- [9] Y. Zing, G. Hu, H.A. Cerdera, S. Chen, T. Braun, Y. Yao, Phys. Rev. E 63 (2001) 026211.
- [10] N. Tsukamoto, S. Miyazaki, H. Fujisaka, Phys. Rev. E 67 (2003) 016212.
- [11] O. Popovych, Yu. Maistrenko, E. Mosekilde, Phys. Rev. E 64 (2001) 026205, see references therein.
- [12] W. Lim, S.-Y. Kim, Phys. Rev. E 71 (2005) 036221.
- [13] A.S. Pikovsky, P. Grassberger, J. Phys. A 24 (1991) 4587; A.S. Pikovsky, Phys. Lett. A 165 (1992) 33.

- [14] H. Fujisaka, T. Yamada, *Prog. Theor. Phys.* 74 (1985) 918;
H. Fujisaka, T. Yamada, *Prog. Theor. Phys.* 75 (1986) 1087;
H. Fujisaka, H. Ishii, M. Inoue, T. Yamada, *Prog. Theor. Phys.* 76 (1986) 1198.
- [15] L. Yu, E. Ott, Q. Chen, *Phys. Rev. Lett.* 65 (1990) 2935;
L. Yu, E. Ott, Q. Chen, *Physica D* 53 (1992) 102.
- [16] N. Platt, E.A. Spiegel, C. Tresser, *Phys. Rev. Lett.* 70 (1993) 279;
J.F. Heagy, N. Platt, S.M. Hammel, *Phys. Rev. E* 49 (1994) 1140;
N. Platt, S.M. Hammel, J.F. Heagy, *Phys. Rev. Lett.* 72 (1994) 3498.
- [17] A. Wolf, J.B. Swift, H.L. Swinney, J.A. Vastano, *Physica D* 16 (1985) 285;
G. Benettin, L. Galgani, A. Giorgilli, J.-M. Strelcyn, *Meccanica* 15 (1980) 9;
A.J. Lichtenberg, M.A. Lieberman, *Regular and Stochastic Motion*, Springer-Verlag, New York, 1983, p. 283.